ACS Catalysis

Perspective

pubs.acs.org/acscatalysis

# Metal–Organic Frameworks for Light Harvesting and Photocatalysis

Jin-Liang Wang,[†] Cheng Wang,[†] and Wenbin Lin*

Department of Chemistry, CB #3290, University of North Carolina, Chapel Hill, North Carolina 27599, United States

**ABSTRACT:** Metal–organic frameworks (MOFs), a new class of crystalline molecular solids built from linking organic ligands with metal or metal-cluster connecting points, have recently emerged as a versatile platform for developing single-site solid catalysts. MOFs have been used to drive a range of reactions, including Lewis acid/base catalyzed reactions, redox reactions, asymmetric reactions, and photocatalysis. MOF catalysts are easily separated from the reaction mixtures for reuse, and yet their molecular nature introduces unprecedented chemical diversity and tunability to drive a large scope of catalytic reactions. This Perspective aims to summarize recent progress on light harvesting and photocatalysis with MOFs. The charge-separated excited states of the chromophoric building blocks created upon photon excitation can migrate over long distances to be harvested as redox equivalents at the MOF/liquid interfaces via electron transfer reactions or can directly activate the substrates that have diffused into the MOF channels for photocatalytic reactions. MOF-catalyzed and photodriven proton reduction, $CO_2$ reduction, and organic transformations will be discussed in this Perspective.

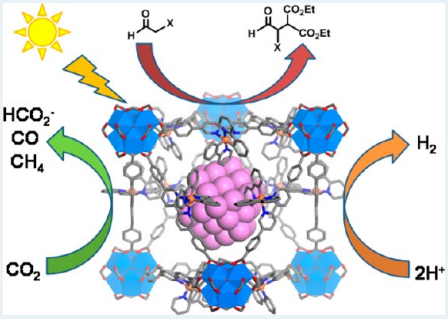


**KEYWORDS:** *metal–organic frameworks, light harvesting, photocatalysis, water splitting, $CO_2$ reduction*

## INTRODUCTION

The ever-increasing global demand for energy has stimulated a new wave of research activities on generating clean and renewable energy using sunlight.[1,2] Light-driven photochemical reactions, such as water splitting and carbon dioxide reduction with water, can transform abundant and renewable sunlight energy into chemical energy in the form of chemical bonds. Such a photochemical transformation of sunlight energy into chemical energy has been practiced by green plants through photosynthesis for hundreds of millions of years.[3] In natural photosynthesis, a complex and intricate system is assembled, via evolutionary selection, by connecting a light-harvesting antenna network, a molecular water oxidation center, and a $CO_2$- or proton-reduction machinery in a hierarchical organization to convert sunlight energy into chemical energy stored in carbohydrates or hydrogen.

Inspired by natural photosynthesis, scientists have long been interested in developing inorganic materials for photochemical conversion of sunlight energy into chemical energy, with the first demonstration of UV light-driven water splitting with semiconducting $TiO_2$ by Fujishima and Honda in 1972.[4] Further developments by Nozik, Domen, Nocera, and others combine different inorganic nanomaterials in hierarchical assemblies to harvest sunlight to drive catalytic water oxidation and proton reduction and have achieved an efficiency of ~4.7% in direct solar-to-fuel conversion based on Nocera's solar water-splitting cell comprising earth-abundant elements (Co and Ni catalysts).[5−11] These multicomponent artificial photosynthesis devices have significantly enhanced the efficiency of light-driven water splitting compared with the Fujishima–Honda cell. Despite these exciting developments on solid state water-splitting devices in recent years, it remains a great challenge to develop a system that can efficiently utilize the full solar spectrum (particularly >600 nm) with high efficiency, acceptable stability, and low cost.

Following the molecular approach adopted by green plants, scientists have also developed various molecular dyes that are capable of converting photons to high-energy redox equivalents as well as molecular catalysts for both water oxidation and proton/$CO_2$ reduction.[12−16] Unlike semiconductor-based water-splitting systems and photosystems I and II,[3] there are not efficient ways of assembling these molecular functional components into hierarchical organizations to convert sunlight energy into chemical energy.

Metal–organic frameworks (MOFs) are a class of crystalline materials that are constructed from well-defined molecular building blocks and metal or metal-cluster connecting nodes. The ability to design micro- or mesoporous extended networks and to incorporate molecular functional components has opened the door for MOFs to many potential applications.[17−27] In particular, MOFs provide a potential platform to organize different molecular components to achieve artificial photosynthesis. An increasing number of papers have appeared in the literature in recent years to indicate that MOFs provide a unique opportunity for integrating different molecular functional components to achieve light harvesting and to drive photocatalytic hydrogen evolution and $CO_2$ reduction.

Sunlight also serves as a means for substrate activation to drive organic transformations that cannot be carried out by conventional means. Photocatalysis has long been proposed as

Received: September 5, 2012
Revised: October 8, 2012
Published: October 24, 2012

   dx.doi.org/10.1021/cs3005874 | ACS Catal. 2012, 2, 2630–2640

an important synthetic methodology for the formation of C−C bonds,[29−32] but its utility is limited by the lack of photon absorption in the solar spectrum by most organic substrates. Recent work using catalytic molecular dyes to absorb lower energy photons for substrate activation has allowed many photocatalytic reactions to be driven with visible light, thus promising a potential renaissance in organic photocatalysis.[33−35] As in any catalytic reactions, heterogenized photocatalysts are of considerable interest for large-scale photocatalytic processes owing to the ability to recover and reuse expensive photocatalysts and to eliminate the contamination of organic products by trace amounts of photocatalysts that often contain heavy metals.[36−38] MOFs serve as an ideal platform to design single-site solid photocatalysts by combining molecular functionality into a solid state material.[39−41] Photoactive MOFs have been used as catalysts for a number of light-driven organic transformations. This Perspective will summarize recent progress on light harvesting and photocatalysis with MOFs. MOF-catalyzed and photodriven proton reduction, $CO_2$ reduction, and organic transformations will be discussed in this Perspective.

**(a). Light-Harvesting with MOFs.** Natural photosynthetic systems integrate highly efficient membrane-bound peripheral chromophores into a network that is wired to a charge separation center.[42] The sunlight energy harvested by the chromophores is funneled to the charge separation center, which itself is a modified dye molecule, to carry out highly efficient photoinduced charge separation. The energetic positive and negative charges (holes and electrons) generated from the charge separation process are then used to drive various chemical transformations. Artificial light-harvesting architectures have been investigated to perform similar tasks. Harvested photon energies have been transferred through a synthesized chromophore network and relayed to charge-separation centers to afford redox-separated states.[43−45] As a result of the well-defined crystal structures of MOFs and controllable chromophore distance via crystal engineering, highly crystalline MOFs have provided a unique opportunity to study energy transfer in such systems.

Lin, Meyer, and co-workers synthesized a phosphorescent MOF (**1**) based on the Ru(II)-(bpy)(4,4′-dcbpy)$_2$ (where bpy is 2,2′-bipyridine and dcbpy is dicarboxy-2,2′-bipyridine) bridging ligand and $Zn^{2+}$ connecting points (Scheme 1). Compound **1** adopts a 2-D bilayer structure with each of the Zn centers coordinating to four carboxylate oxygen atoms of $\mathbf{L_{1\text{-}Ru}}$ ligands in a tetrahedral geometry. Compound **1** has strong absorption in the visible region and can be readily excited to their long-lived triplet metal-to-ligand charge transfer ($^3$MLCT) states.[47] The Os(II)-bpy analog ($\mathbf{L_{1\text{-}Os}}$) was doped into the framework structure to study energy migration processes in this MOF by detecting the Ru-to-Os energy transfer. Time-resolved emission studies were performed with a two-photon excitation at 850 nm (Figure 1a). The lifetimes of Ru(II) excited states in the Os-doped **1** decreased progressively with increasing Os doping from 0.3 to 2.6 mol % (Figure 1b). Convincingly, an initial growth in Os emission was observed, giving strong evidence to the Ru-to-Ru and Ru-to-Os energy transfer in **1** (Figure 1b). The $^3$MLCT excited states are estimated to undergo an average of 50 Ru-to-Ru hops in their lifetimes. The photophysical results demonstrated rapid, efficient energy migration in these isomorphous MOFs.

Lin, Meyer, and co-workers then probed the charge separation ability of MOF **1** and MOF **2** that is built from

**Scheme 1. Synthesis of Phosphorescent MOFs 1 and 2 and Chemical Structures of Various Redox Quenchers**[a]

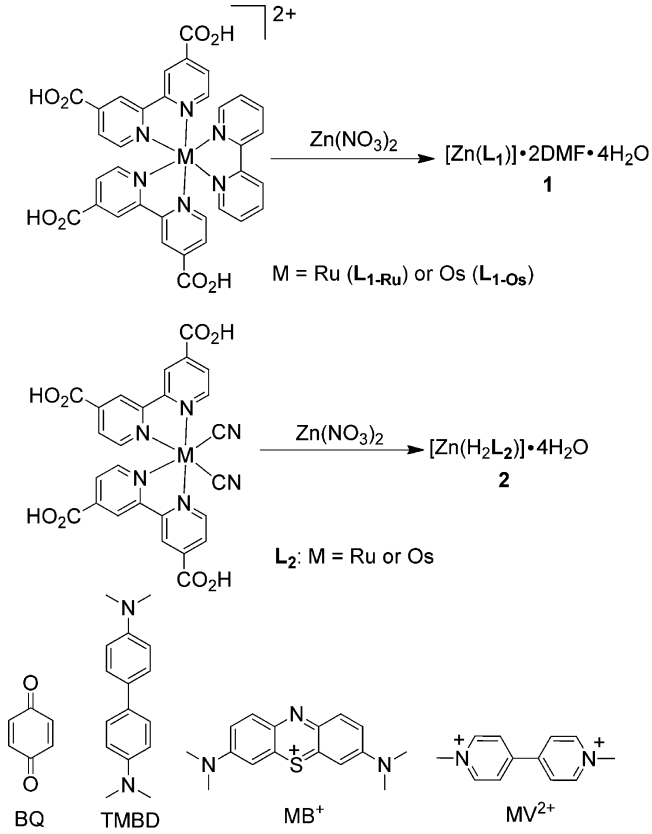


[a]BQ (1,4-benzoquinone), TMBD (*N,N,N′,N′*-tetramethylbenzidine), MB (methylene blue), and MV (methyl viologen).

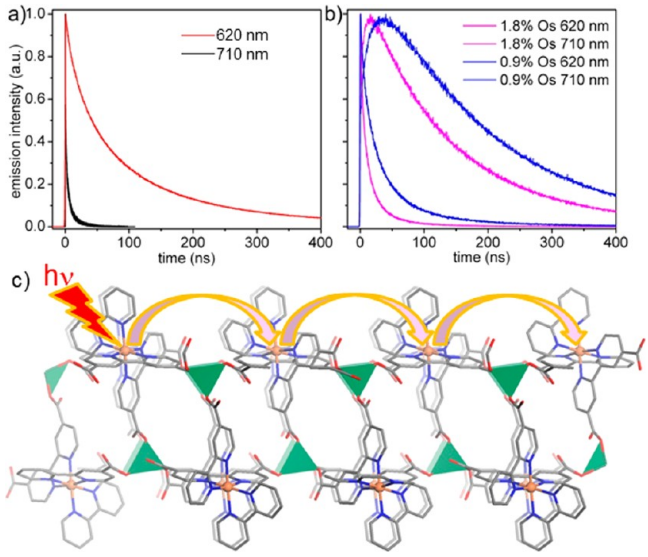


**Figure 1.** (a) Transient emission decay profiles for **1** and **1-Os** monitored at 620 and 710 nm, respectively, following two-photon excitation at 850 nm. (b) Transients for 1.4 and 2.6 mol % Os-doped **1** at 620 and 710 nm with emission at 620 nm dominated by Ru(II)* and at 710 nm by Os(II)*. (c) Schematic depicting the hopping of the Ru(II)*-bpy excited states in these isomorphous MOFs. Reprinted with permission from ref 47. Copyright 2011, American Chemical Society.


dx.doi.org/10.1021/cs3005874 | *ACS Catal.* 2012, 2, 2630−2640

the $Ru(II)(CN)_2(dcbpy)_2$ bridging ligand by redox luminescence quenching.[46] Quenching experiments were carried out with stirred suspensions of the MOFs in degassed acetonitrile and the oxidative quencher (1,4-benzoquinone, BQ) or the reductive quencher (*N*,*N*,*N*′,*N*′-tetramethylbenzidine, TMBD). The concentrations of MOFs were about 40 $\mu$M (based on Ru) as determined by the UV−vis absorption measurement after digestion with tetrabutylammonium hydroxide. As shown in Figure 2, the luminescence of microcrystals of **2** can be

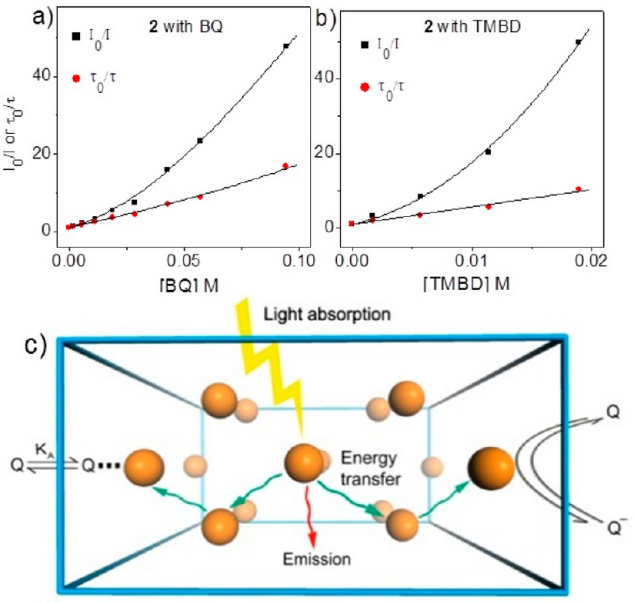


**Figure 2.** (a,b) Steady-state (black) and time-resolved (red) Stern−Völmer quenching analysis of **2** with BQ (a) or TMBD (b). The Stern−Völmer plot of $I_0/I$ represents a sum of static and dynamic (diffusional) quenching. The plotted emission intensity was integrated from 550 to 850 nm. The Stern−Völmer plot of $\tau_0/\tau$ represents the dynamic component of quenching. Lifetime data were obtained when excited at 485 nm and monitored at the emission maximum at 620 nm. Emission transients were fit to the triexponential decay to obtain weighted lifetimes. (c) Schematic showing the light-harvesting process in MOF microcrystals as a result of a rapid energy migration over several hundred nanometers followed by efficient electron transfer quenching at the MOF/solution interface. Reprinted with permission from ref 46. Copyright 2011, American Chemical Society.

efficiently quenched by either BQ or TMBD as a result of efficient light-harvesting and excited-state electron transfer in these MOFs. For example, >98% of the Ru(II)* emission from the crystal was quenched with 0.1 M BQ quencher. The experimental data were fitted with a model considering both the static and dynamic components of the quenching process, revealing a rapid energy migration over several hundred nanometers, followed by efficient electron transfer quenching at the MOF/solution interface.[46] These results indicate that MOF microcrystals can provide an ideal platform for designing molecular solids for light harvesting.

More recently, Lin, Meyer, and co-workers observed an amplified quenching for **2** with methylene blue as the quencher. A 7000-fold enhancement of Stern−Völmer quenching constant was obtained as compared with a model complex, $Ru(bpy)_2(CN)_2$, as a result of strong, noncovalent interactions between the MOF surface and cationic quencher molecules coupled with rapid energy transfer through the whole microcrystal (Figure 3).[48] This work suggests that phosphorescent MOFs should provide a promising platform for designing highly sensitive and selective sensors by taking advantage of the tunability and crystalline structures of MOFs.

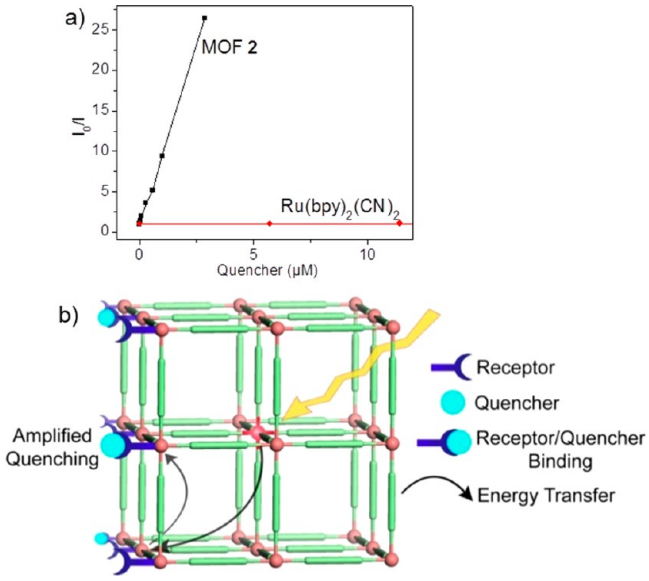


**Figure 3.** (a) Stern−Völmer analysis of **2** with added $MB^+$ by steady-state emission measurements and of $Ru(bpy)_2CN_2$ by time-resolved emission measurements. (b) Schematic showing amplified quenching of MOF luminescence as a result of long-distance intra-MOF energy transfer and efficient electron transfer quenching at the interface. Reprinted with permission from ref 48. Copyright 2012, American Chemical Society.

**(b). Proton Reduction with MOFs.** During the past decade, various inorganic semiconductor and molecular complexes have been developed as photocatalysts for the splitting of water into hydrogen and oxygen using sunlight energy.[8,49−52] A few examples of MOFs have been used either as photosensitizers or as catalysts for proton reduction reaction with sacrificial reductants. Mori and co-workers first reported in 2009 a porous MOF with the formula of $[Ru_2(p\text{-}BDC)_2]_n$ (BDC = benzenedicarboxylate) that is capable of visible-light-driven proton reduction with $Ru(bpy)_3^{2+}$ as a photosensitizer, $MV^{2+}$ as an electron relay, and $Na_2EDTA$ as a sacrificial reductant.[53] $[Ru_2(p\text{-}BDC)_2]_n$ was constructed from $Ru_2(carboxylate)_4$ paddlewheel SBUs and BDC linker, leading to a 2-D square grid sheet structure with 1-D channels that run perpendicular to the layers. The resultant MOF is stable in air and water. The catalytic reaction in water gives a turnover number of 8.16 for hydrogen evolution (based on the amount of Ru in $[Ru_2(p\text{-}BDC)_2]_n$) after 4 h of irradiation. The reaction cycle is believed to start with the photoinduced charge transfer between the excited state of $Ru(bpy)_3^{2+}$ and the electron relay ($MV^{2+}$) to yield $Ru(bpy)_3^{3+}$ and $MV^+$ (Figure 4). $MV^+$ then transfers the electron to the $Ru_2(carboxylate)_4$ paddlewheel SBU in $[Ru_2(p\text{-}BDC)_2]_n$, which reduces water to hydrogen. The reduction of $Ru(bpy)_3^{3+}$ by $Na_2EDTA$ regenerates the initial photosensitizer. The nature of the active proton reduction catalyst, however, was not delineated in this work.

García and co-workers used highly stable Zr-containing MOFs (UiO-66 and UiO-66($NH_2$)), which were originally developed by Lillerud and co-workers,[54] for water reduction in 2010. The MOFs were built from the *p*-BDC or 2-aminoterephthalate (amino-BDC) linear linker and the $Zr_6(O)_4(OH)_4(CO_2)_{12}$ SBU.[55] The high stability of these


dx.doi.org/10.1021/cs3005874 | *ACS Catal.* 2012, 2, 2630−2640

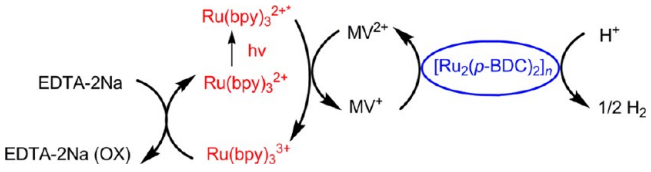


**Figure 4.** Proposed photocatalytic cycle of hydrogen evolution from water using the $[Ru_2(p\text{-BDC})_2]_n$, $Ru(bpy)_3^{2+}$, $MV^{2+}$, and $Na_2EDTA$ combination under visible light irradiation. Reprinted with permission from ref 53. Copyright 2009, Royal Society of Chemistry.

MOFs in water encouraged the investigation of their potential in photocatalytic water reduction. The MOF-catalyzed hydrogen generation was evaluated with a UV irradiation (>300 nm) and methanol as the sacrificial electron donor. The presence of amino group in the terephthalate introduced an absorption band at >300 nm, making the photocatalysis possible. Platinum nanoparticles were also added to the reaction mixture as a cocatalyst for hydrogen evolution. The need for UV photons in this work, however, limits the utility of proton reduction with the UiO-66 MOF.

Because the visible-light-driven photocatalytic hydrogen evolution often requires both a phosphor to harvest photons and a cocatalyst, such as Pt nanoparticles, to catalyze the production of hydrogen, it is beneficial to assemble the two components in the same framework to catalyze water reduction. In early 2012, Lin and co-workers reported a novel synergistic hydrogen evolution system based on the Pt nanoparticle@MOF assemblies.[56] $Zr_6(\mu_3\text{-O})_4(\mu_3\text{-OH})_4$(biphenyldicarboxylate)$_{5.94}$(bis(4-phenyl-2-pyridine)-(5,5′-dicarboxylate)-2,2′-bipyridine)-iridium(III) chloride)$_{0.06}$ (**3**) was prepared by doping the bis(4-phenyl-2-pyridine)-(5,5′-dicarboxylate)-2,2′-bipyridine)-iridium(III) chloride ($\mathbf{L_3}$) into the parent UiO-67 framework with the biphenyldicarboxylate as the bridging ligand at about 2 wt % loading (Figure 5). The noninterpenetrated UiO framework, **4**, was constructed from the bis(4-phenyl-2-pyridine)(5,5′-di(4-phenylcarboxylate)-2,2′-bipyridine)-iridium(III) chloride ($\mathbf{L_4}$) bridging ligand and $Zr_6(\mu_3\text{-O})_4(\mu_3\text{-OH})_4$(carboxylate)$_{12}$ SBU.

The Pt nanoparticle@MOF assemblies were constructed via in situ MOF-mediated photodeposition of Pt nanoparticles inside the MOF channels. Because **4** has a larger void space and a higher concentration of the Ir-photosensitizer, much larger amounts of Pt nanoparticles were loaded into the channels of **4** in comparison with **3**. Both Pt@MOF assemblies are highly active photocatalysts for proton reduction with triethylamine as the sacrifical reductant. Under the illumination of a 450 W Xe lamp with a 420 nm long-pass filter for 48 h, Pt@**3** and Pt@**4** exhibited a total turnover number (TON) of 3400 and 7000 based on Ir complexes, respectively (Figure 6). These TONs are almost 5 times higher than those of the homogeneous control as a result of the facile eletron transfer from the photoreduced Ir complexes to the entrapped Pt nanoparticles. Moreover, the catalysts could be recycled and reused at least three times. Nearly 25% Ir complexes of MOFs leached into solution after the 48 h reactions, presumably due to the photodecomposition of the Ir photosensitizers. This work provides an interesting pathway to hierarchically integrate multiple functional components into the same MOF scafford to afford highly efficient photocatalysts.

Porphyrins are attractive building blocks for MOF construction due to their high thermal stability and interesting photophysical properties.[57−59] Rosseinsky and co-workers recently reported the synthesis of a water-stable porous porphyrin MOF (Al-PMOF) by treating $AlCl_3$ with free-base meso-tetra(4-carboxyl-phenyl)porphyrin under hydrothermal conditions.[60] The four carboxylate groups of each porphyrin linker of the Al-PMOF coordinate to eight Al centers, while the metal centers form an $Al(OH)O_4$ chain bridged by carboxylate oxygen atoms and $\mu_2$-$OH^-$ moieties. The connectivity of the

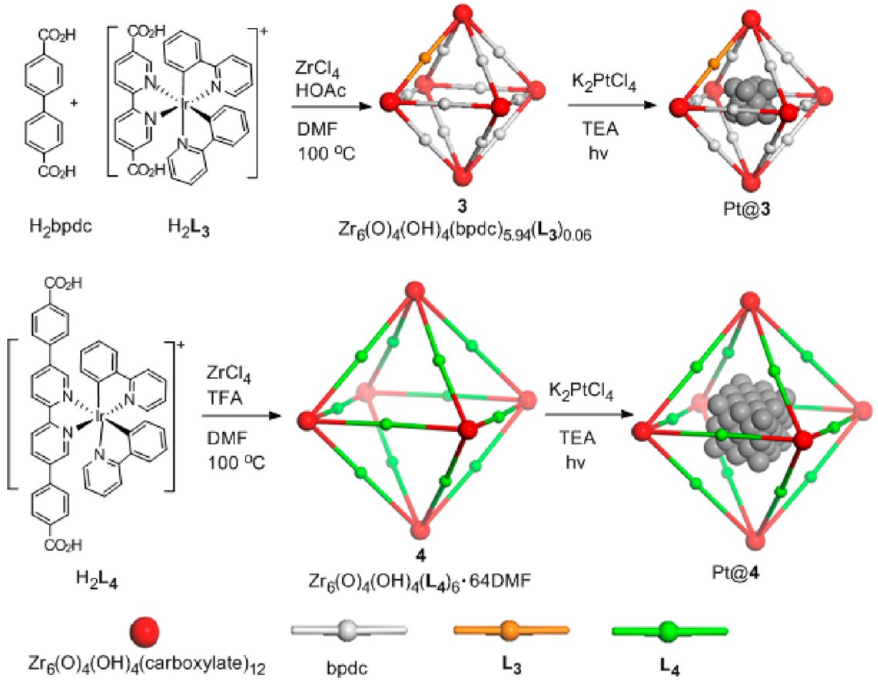


**Figure 5.** Synthesis of phosphorescent zirconium carboxylate MOFs and subsequent loading of Pt NPs inside MOFs **3** and **4**. Reprinted with permission from ref 56. Copyright 2012, American Chemical Society.


dx.doi.org/10.1021/cs3005874 | ACS Catal. 2012, 2, 2630−2640

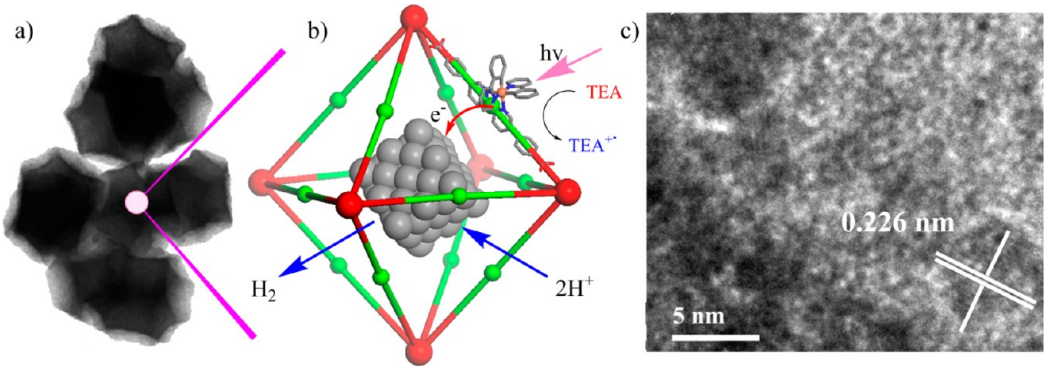


**Figure 6.** (a) TEM images of Pt@4. (b) The synergistic photocatalytic hydrogen generation process via photoinjection of electron from the light-harvesting MOF on to the Pt NPs. (c) HRTEM images of a powdery sample of Pt@4 that shows the lattice fringes of the Pt particles, with *d*-spacing matching that of the Pt{111} plane. Reprinted with permission from ref 56. Copyright 2012, American Chemical Society.

Al-PMOF is similar to that of MIL-60.[61] The Al-PMOF is photoactive with visible light excitation and has been evaluated for the visible-light-driven hydrogen generation from water (Figure 7). When the proton reduction was carried out using

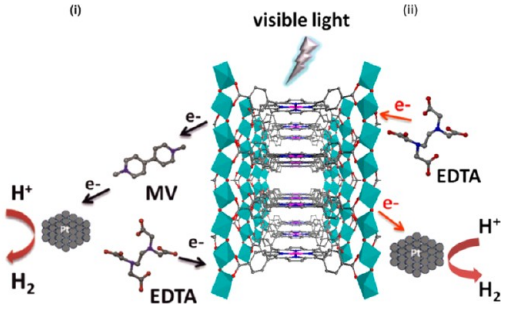


**Figure 7.** Proposed photocatalytic reactions using Al-PMOF in the presence of MV (i) or in the absence of MV (ii). Reproduced with permission from ref 60. Copyright 2012, Wiley-VCH.

the Al-PMOF/$MV^{2+}$/EDTA/Pt system that is analogous to the strategy used by Mori et al., low activity was found with much less than stoichiometric amounts of $H_2$ generated for each porphyrin strut. The authors believed that the low activity resulted from slow diffusion of methyl viologen through the Al-PMOF channels, which leads to ineffective electron transfer from the reduced viologen radical to Pt nanoparticles. Interestingly, when methyl viologen was removed from the reaction mixture, the rate and quantum yield of hydrogen generation increased to about 200 $\mu$mol $g^{-1}$ $h^{-1}$ and about 0.1%, respectively, more than 1 order of magnitude higher than the MV-based approach. In the MV-free approach, ~0.7 $H_2$ molecules were generated for each porphyrin strut in 6 h of photocatalytic reaction. The Al-PMOF frameworks remained intact after the photocatalytic reaction, as revealed by powder XRD and further confirmed by no detectable leaching of the porphyrin strut into the solution. The ability to postsynthetically metalate the porphyrin strut in this system should allow further tuning of the photocatalytic activity to increase hydrogen generation TONs.

**(c). Carbon Dioxide Reduction with MOFs.** In photosystem I, $CO_2$ is reduced by NADPH generated in the photochemical process.[62] Photoreduction of $CO_2$ into valuable organic compounds on a large scale not only harvests energy from sunlight for human consumption, but also helps balance the $CO_2$ level in the atmosphere.[63] A number of molecular compounds, semiconducting materials, and metal-incorporated zeolites have been developed as photocatalysts for $CO_2$ reduction.[64−66]

$Re(I)(CO)_3(bpy)X$ complexes have recently been examined for selective reduction $CO_2$ into CO.[67] These Re complexes, however, decompose during the catalytic trunovers and lose their activities. Two mechanisms involving either bimolecular activation or a unimolecular pathway have been proposed for the $CO_2$ reduction reactions. Lin and co-workers reported in 2011 the incorporation of $[Re(I)(CO)_3(5,5,'\text{-dcbpy})Cl]$ (at 4 wt % loading) into the UiO-67 framework to afford **5** (Scheme 2).[68] Compound **5** was synthesized by taking advantage of the matching ligand lengths of bpdc and $\mathbf{L_5}$ and exhibited the same PXRD as the parent UiO-67 (Figure 8c). The photocatalytic $CO_2$ reduction activity of **5** was investigated in $CO_2$-saturated acetonitrile using triethylamine as the sacrificial reducing agent under a 450 W Xe-lamp. Compound **5** selectively reduced $CO_2$ to CO with a TON of 10.9, 3 times higher than that of the homogeneous complex (Figure 8a). Importantly, the molar amount of CO was about 10 times higher than that of $H_2$ generated during the first 6 h. No formic acid or methanol was detected during the photocatalytic reactions. Lin and co-workers also tested the recyclability of **5** in light-driven carbon

**Scheme 2. Synthesis of 5 by Doping $[Re^{I}(CO)_3(5,5,'\text{-dcbpy})Cl]$ into the UiO-67 Framework**

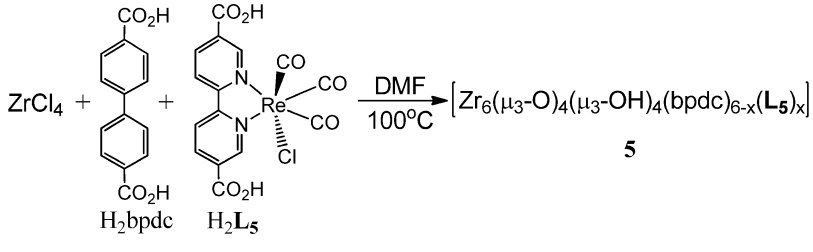



dx.doi.org/10.1021/cs3005874 | ACS Catal. 2012, 2, 2630−2640

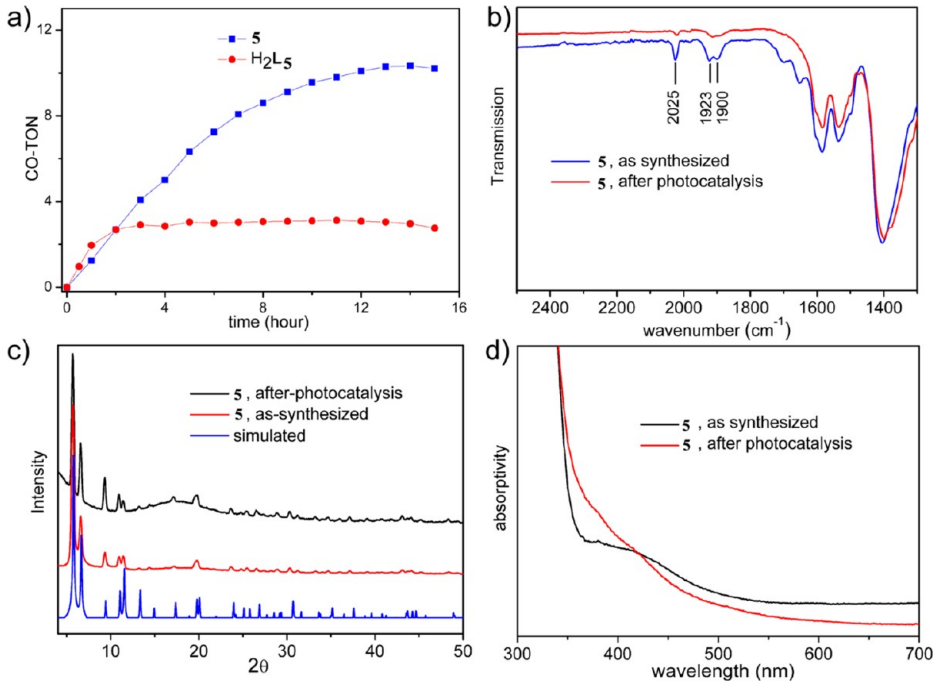


**Figure 8.** (a) Plots of CO evolution turnover number versus time in the photocatalytic $CO_2$ reduction with **5** and the homogeneous control. (b) FT-IR of **5** before and after photocatalysis. (c) PXRD patterns of **5** before and after photocatalysis. The simulated PXRD for the UiO-67 is also shown. (d) UV−vis diffuse reflectance spectra of **5** before and after photocatalysis. Reprinted with permission from ref 68. Copyright 2011, American Chemical Society.

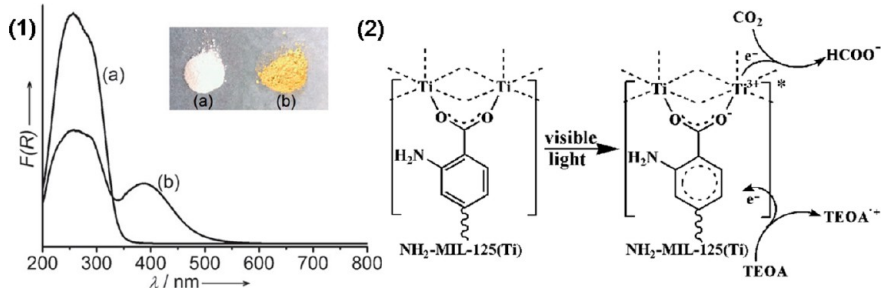


**Figure 9.** (1) Absorption spectra of MIL-125(Ti) (curve a) and $NH_2$-MIL-125(Ti) (curve b) (2) Proposed mechanism for phtotocatalytic $CO_2$ redution of $NH_2$-MIL-125(Ti). Reproduced with permission from ref 69. Copyright 2012, Wiley-VCH.

dioxide reduction. The recovered catalyst became inactive for CO generation, but still showed slight activity for $H_2$ generation. PXRD of the recovered solid indicated that the UiO-67 framework remained intact and did not dissolve into the solution (Figure 8c). As shown in Figure 8d, the recovered solid lost the diagnostic MLCT absorption peak (~412 nm) of the $Re(I)(CO)_3(bpy)Cl$ complex (Figure 8d) and exhibited a drastically decreased intensity of CO stretching vibrations in comparison to the as-synthesized **5** (Figure 8b). Taken together, **5** lost its activity owing to the detachment of the Re-carbonyl moieties from the dcbpy backbones of the framework of **5** during the photocatalytic reactions. In addition, because the biomolecular pathways are inoperative in **5** as a result of the site isolation of $[Re(I)(CO)_3(5,5,'\text{-dcbpy})Cl]$ complexes, the observed photocatalytic activity of **5** lends strong support for the unimolecular pathway of photocatalytic $CO_2$ reduction. This work thus not only demonstrated the ability to carry out photocatalytic $CO_2$ reduction with a MOF but also provided important mechanistic insights into $CO_2$ reduction with $Re^{I}(CO)_3(bpy)X$ complexes.

Recently, Li and co-workers reported a photoactive catalyst $Ti_8O_8(OH)_4(bdc\text{-}NH_2)_6$ ($NH_2$-MIL-125(Ti)) using 2-amino-BDC as the linker for $CO_2$ reduction under visible irradiation.[69] The presence of $NH_2$ in the linker does not affect the structure of MIL-125(Ti) and introduces an extra visible light absorption band that extends to 550 nm (Figure 9). The ability of $NH_2$-MIL-125(Ti) to undergo photoinduced charge separations was recently demonstrated by García, Serre, and co-workers.[70] The photocatalytic reduction of $CO_2$ into formate anion $HCO_2^-$ was carried out in MeCN with triethanolamine (TEOA) as a sacrificial agent under visible irradiation. Upon light illumination on the MOF, $Ti^{4+}$ can be reduced to $Ti^{3+}$ by the ligand. When $CO_2$ was introduced into the suspension, the reduction of $CO_2$ by $Ti^{3+}$ to $HCOO^{2-}$ was observed in the presence of TEOA as an electron donor. Compared with the parent MIL-125(Ti), $NH_2$-MIL-125(Ti) showed slightly higher photocatalytic activity (the amount of $HCOO^{2-}$ reached 8.14 $\mu$mol, and the corresponding TON based on per Ti center was ~0.03 in 10 h) due to its higher light absorption in the visible spectrum. The framework of $NH_2$-MIL-125(Ti) remained intact during the photocatalytic reduction of $CO_2$.


dx.doi.org/10.1021/cs3005874 | ACS Catal. 2012, 2, 2630−2640

**(d). Photocatalytic Organic Reactions with MOFs.** The use of visible-light photoredox catalysts to initiate organic transformations has been investigated since the 1970s.[71] Although not widely used by the mainstream synthetic organic community, photocatalysis has evolved into a powerful and efficient tool in the past few years, in part as a result of the successful employment of various dye molecules.[16,72] MOFs have recently been examined as photocatalysts to drive a number of organic transformations.

Photodegradation of organic substrates is one of the most explored area of photocatalysis.[73] The $Zn_4O(BDC)_6$ MOF, commonly referred to as MOF-5, has an absorption spectrum that extends to 400 nm and can undergo photochemical processes upon photoexcitation of the organic linker. In 2007, Garcia et al. reported the generation of charge-separated excited states upon photoexcitation of MOF-5 and the reduction of an electron acceptor, such as methyl viologen dichloride, with photogenerated electrons or oxidation of an electron donor, such as *N*,*N*,*N*′,*N*′-tetramethyl-p-phenylenediamine, with photogenerated holes.[74] MOF-5 showed photocatalytic activity for the degradation of phenol comparable to that of the P-25 titanium dioxide standard. As shown in Figure 10, the authors

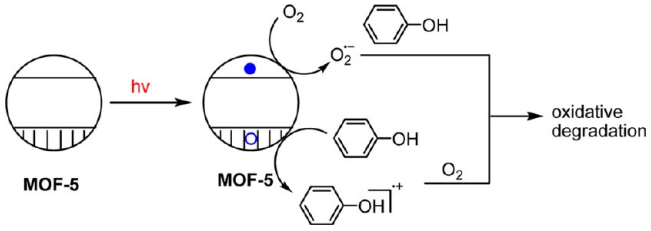


**Figure 10.** The proposed mechanism for photodegradation of phenol with MOF-5. Reproduced with permission from ref 74. Copyright 2012, Wiley-VCH.

proposed the initiation of photodegradation via the formation of a radical cation by electron transfer from phenol to the photogenerated hole in MOF-5 or the generation of active oxygen species from the reaction between the photogenerated electrons and molecular oxygen. However, the utility of MOF-5 as a photocatalyst is limited by its susceptibility toward hydrolysis.

Methyl orange is one of the stable azo dyes and a common environment pollution source because of its resistance to degradation. In 2011, Chen and co-workers reported that a doubly interpenetrated porous MOF $Zn_4O$ (2,6-naphthalenedicarboxylate)$_3$(DMF)$_{1.5}$($H_2O$)$_{0.5}$·4DMF·7.5$H_2O$ (UTSA-38) with an absorption band of 2.85 eV can be used to degrade methyl orange under visible light (Figure 11).[75] The authors speculated that the photodecomposition is initiated via the photoinduced reduction of $O_2$ to $\cdot O_2^-$ radical, which quickly transforms into a hydroxyl radical (·OH). The hydroxyl radical then decomposes methyl orange. Importantly, these MOF catalysts can be readily recovered and reused several times.

Li and co-workers recently reported a family of MOFs with conjugated 1,2,4,5-benzenetetracarboxylic acid (btec), 4,4′-bis(1-Imidazolyl)biphenyl (bimb), and corresponding metal ions for visible-light-driven heterogeneous photocatalysis.[76] Some of them, such as $[Cd(btec)_{0.5}(bimb)_{0.5}]_n$ (**6**), exhibited higher photocatalytic activities than that of commercial $TiO_2$ (Degussa P-25) under visible irradiation (Figure 12). The organic dye X3B was used as a model pollutant. They also found that the relatively narrow bandgap improved the activity of photodegradation. A synergistic effect of $H_2O_2$ and MOFs on the photo degradation of X3B suggested that hydroxyl radicals (·OH) can effectively oxidize the dye molecules; thus, the formation rate of ·OH is an important factor for the photocatlytic performance. However, the generated ·OH also has the potential to decompose the organic ligand of the MOF, potentially leading to framework degradation.

Photodegradation of organic pollutants is an important area, but typically involves only the generation of reactive oxygen species. Photocatalytic organic transformations often require more elaborate control of the reaction cycles, thus presenting a greater challenge in MOF photocatalyst design. Molecular phosphors $Ru(bpy)_3Cl_2$ and $Ir(ppy)_2(bpy)PF_6$ (ppy =2-phenylpyridine) have been used as photoredox catalysts in various interesting organic reactions and functional group transformations.[33,77,78] It is desirable to develop corresponding reusable heterogeneous photocatalysts due to the need to recycle expensive precious metals in these catalysts.

Lin and co-workers have recently prepared highly stable and robust UiO-67 MOFs that are doped with $Ir(ppy)_2$(5,5′-dcbpy)Cl and $Ru(bpy)_2$(5,5′-dcbpy)$Cl_2$ at about 3 wt % loadings (Scheme 3).[68] Aza-Henry reactions of tertiary amines, aerobic oxidative couplings of amines, and photo-oxidations of sulfides were chosen as model reactions to demonstrate the photocatalytic activities of these MOFs. For example, aza-Henry reactions were carried out with various tetrahydroisoquinoline derivatives as the amine substrates and air as the oxidant. The reactions were performed in $CH_3NO_2$ at 1 mol %

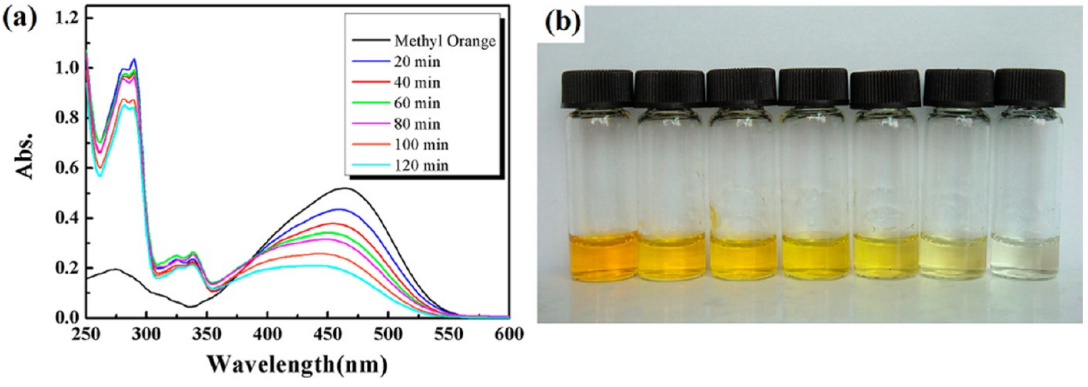


**Figure 11.** UV−vis absorption spectra and photograph of methyl orange solution degraded by UTSA-38 after UV−vis light irradiation for different times. Reprinted with permission from ref 75. Copyright 2011, Royal Society of Chemistry.


dx.doi.org/10.1021/cs3005874 | *ACS Catal.* 2012, 2, 2630−2640

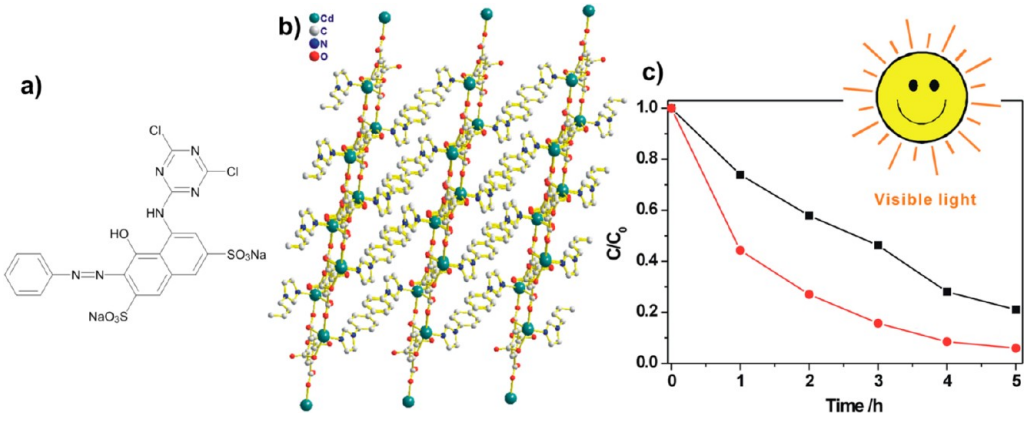


**Figure 12.** (a) The chemical structure of X3B, (b) The 3D structure of **6**, and (c) concentration changes of X3B as a function of irradiation time under a halogen lamp in the presence of **6** (black) or **6** + $H_2O_2$ (red). Reprinted with permission from ref 76. Copyright 2012, American Chemical Society.

**Scheme 3. Synthesis of Phosphor-Doped UiO-67 Frameworks 7 and 8.**

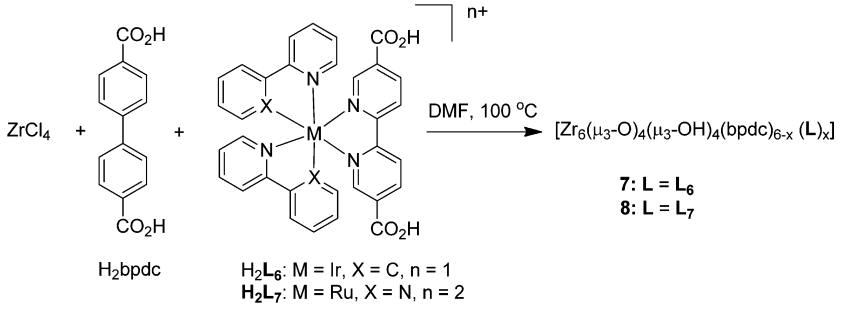


catalyst loading with a 26 W fluorescent lamp as the light source. MOFs **7** and **8** effectively catalyzed aza-Henry reactions between $CH_3NO_2$ and phenyl-, *p*-bromophenyl-, and *p*-methoxyphenyl-substituted tetrahydroisoquinoline in 59−97% conversion yields (Table 1).[78] MOF **8** efficiently catalyzed aerobic oxidative couplings of various benzylamine at 1 mol % catalyst loading under 300 W Xe lamp and 60 °C. Conversion yields of 46−90% were obtained after 3 h of reactions (Table 2). MOF **8** also catalyzed selective aerobic oxidation of thioanisole to methyl phenylsulfoxide in 73% yield with methanol as the solvent and $O_2$ as the oxidizing agent in the presence of light. It is possible that all reactions were mediated by photochemically generated singlet oxygen due to the absence of size selectivity of those reactions. In addition, both MOF catalysts exhibited excellent reusability and retained crystallinity after the photocatalytic reactions. No leaching of precious metals was observed during three reuse cycles.

**Table 1. Photocatalytic aza-Henry Reactions with MOFs 7 and 8**

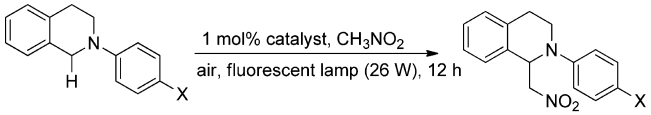


R1 X = H
R2 X = Br
R3 X = $CH_3O$

P1 X = H
P2 X = Br
P3 X = $CH_3O$

| compds | product | 7 | 8 | $Et_2L_6$[a] | $Et_2L_7$[a] |
|---|---|---|---|---|---|
| R1 | P1 | 59% | 86% | 99% | 97% |
| R2 | P2 | 62% | 68% | 90% | 88% |
| R3 | P3 | 96% | 97% | >99% | >99% |

[a]Diethyl esters of $L_6$ and $L_7$ ($Et_2L_6$ and $Et_2L_7$) were used as homogeneous controls.

**Table 2. Photocatalytic Aerobic Amine Coupling Reaction Based on 8**

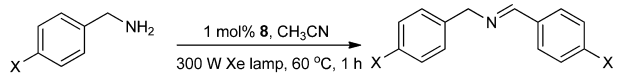


R4 X = H
R5 X = $CH_3$
R6 X = $OCH_3$

P4 X = H
P5 X = $CH_3$
P6 X = $OCH_3$

| compd | product | no light | no catalyst | $Et_2L_7$ | 8 | reused 8 |
|---|---|---|---|---|---|---|
| R4 | P4 | 6% | 8% | 96% | 83% | 80% |
| R5 | P5 | | | | 90% | |
| R6 | P6 | | | | 46% | |

Metalloporphyrin-based MOFs showed light-harvesting and interesting photocatalytic activities.[79,80] Wu and co-workers employed the photoactive tin porphyrin ($Sn^{IV}$TPyP) bridging ligand to construct 3-D porous MOF (Sn-MOF). The Sn-MOF was built from linking the $Sn^{IV}$TPyP struts by the Zn atoms, which was further pillared by formate groups to form a 3D porous network.[81] The photoactive sites in this MOF were immobilized in the channel walls and showed high photocatalytic performance for photo-oxygenation of 1,5-dihydroxynaphthalene to 5-hydroxynaphthalene-1,4-dione and various sulfides into sulfoxides, using $O_2$ as the oxidant. Moreover, Sn-MOF can be recovered by filtration and subsequently reused several times without reducing the efficiency.


dx.doi.org/10.1021/cs3005874 | ACS Catal. 2012, 2, 2630−2640

Chiral porous MOFs are good platforms for heterogeneous asymmetric catalytic reactions because they impose size and shape restrictions by fine-tunable channels and high enantioselectivity by imbedded, well-defined chiral functional species.[82] Combination of an asymmetric organocatalyst with a photoactive MOF can potentially merge the photocatalytic and organocatalytic cycles to lead to highly efficient and setereoselective photocatalysis.[35,83] Duan and co-workers incorporated a stereoselective organocatalyst L or D-pyrrolidine-2-yl-imidazole (PY1) and a photoactive triphenylamine moiety into the same MOF (Zn-PYI1 or Zn-PYI2) scafford (Figure 13). The chiral MOFs were used as heterogeneous catalysts for light-driven asymmetric $\alpha$-alkylation of aldehydes under a fluorescent lamp (26 W).[84] The MOF could adsorb 1.5 equiv of diethyl 2-bromomalonate per triphenylamine group and about 1 equiv of phenylpropylaldehyde per proline moiety. The photocatalytic reaction between these two substrates afforded a high yield (74%) and excellent enantioselectivity (92%) (Table 3). It was speculated that the excited state of triphenylamine acts as a reductant to transfer an electron from the MOF to diethyl 2-bromomalonate to afford an electrophilic radical. Meanwhile, the asymmetric highly $\pi$-nucleophilic enamine from condensation of aldehyde and proline attacked the electron-deficient radical to form the new chiral center. Control experiments using lanthanide-based metal−organic framework Ho-TCA (TCA = tricarboxy-triphenylamine) or MOF-150 as photocatalyst with the same chiral adducts gave good yields but much lower ee values in comparison with Zn-PYI1. These results indicated that the combination of both a photosensitizer and an asymmetric organocatalyst into one single framework can lead to a highly stereoselective, photocatalytic MOF.

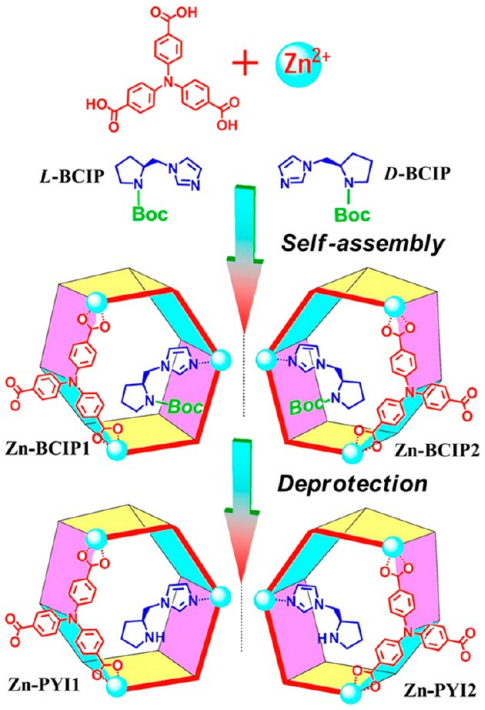


**Figure 13.** Schematic representation of mirror image structures of Zn-BCIP1 and Zn-BCIP2 and their deprotected forms Zn-PYI1 and ZnPYI2. Reprinted with permission from ref 84. Copyright 2012, American Chemical Society.

## CONCLUSIONS AND OUTLOOK

MOFs have emerged as an interesting platform to engineer molecular solids for light-harvesting and photocatalysis. Very impressive results have been obtained in the last 3−4 years with the realization of light-driven hydrogen evolution, $CO_2$ reduction, and organic reactions with photoactive MOFs. Compared with other photocatalytic systems, photoactive MOFs have several advantages: (1) The heterogeneous nature of these photocatalysts allows facile catalyst recycle and reuse. (2) The modular nature of MOF synthesis allows for fine-tuning and rational design of these photocatalysts at the molecular level. (3) The well-defined crystalline structure of MOFs is beneficial to the characterization and study of structure−property relationship of these solid photocatalysts. (4) Intrinsic porosity of many of the MOFs facilitates the diffusion of substrates and products through the open channels. (5) The versatile methods of MOF synthesis, including but not limited to, solvothermal, vapor diffusion, and emulsion-assistant precipitation, provides a high degree of morphology control. Catalyst organization on the nano/micro scale can play an important role in photocatalytic applications. (6) MOFs

**Table 3. Conversions and the ee Values (in the parentheses) of the Photocatalytic $\alpha$-Alkylation of Aldehydes[a]**

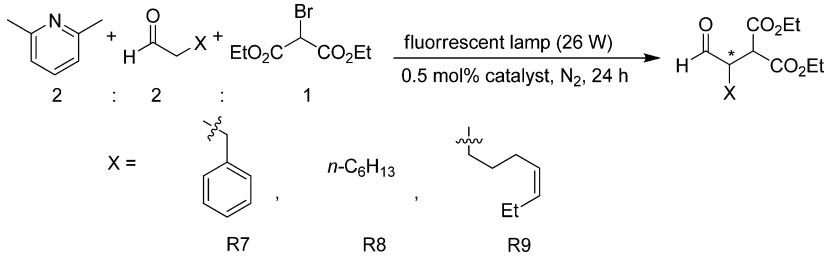


| catalyst | R7 | R8 | R9 |
|---|---|---|---|
| Zn-PYI1 | 74 (+92) | 65 (+86) | 84 (+92) |
| Zn-PYI2 | 73 (−81) | 61 (−78) | 85 (−89) |
| Ho-TCA/L-PYI[a] | 86 (+20) | 90 (+21) | 93 (+20) |
| Ho-TCA/D-PYI[a] | 85 (−21) | 90 (−20) | 95 (−20) |
| MOF-150/L-PYI[a] | 67 (+21) | 78 (+24) | 80 (+20) |
| MOF-150/D-PYI[a] | 62 (−22) | 73 (−22) | (−21) |

[a]In the presence of additional chiral D/L-**PYI** (20 mol %).


dx.doi.org/10.1021/cs3005874 | ACS Catal. 2012, 2, 2630−2640

provide a potential platform to organize different molecular components in an ordered manner to achieve artificial photosynthesis. Although photocatalytic hydrogen generation and $CO_2$ reduction have been achieved with a number of MOFs, all of these systems require the use of sacrificial agents. To achieve hydrogen generation and $CO_2$ reduction without relying on sacrificial agents, an effective water oxidation catalyst must be incorporated into these MOFs. Lin and co-workers recently demonstrated the ability to integrate molecular water oxidation catalysts into MOFs.[58] Much more work, however, is needed in this area to achieve efficient photocatalytic water splitting and $CO_2$ reduction with water using MOF assemblies.

Many MOFs tend to have modest hydrolytic and thermal stabilities, which limit their practical applications in solar energy utilization, especially for water splitting and $CO_2$ reduction with water. A number of MOFs based on hard metal ions, such as $Zr^{4+}$, $Ti^{4+}$, and $Fe^{3+}$ with carboxylate linkers (e.g., UiOs, MIL-140, -125, -101) or soft metal ions, such as $Zn^{2+}$, with imidazolate linkers (e.g., ZIFs) have, however, been shown to exhibit high stability in aqueous solutions. The development of such stable MOFs can overcome the instability issue that can plague other MOFs in many applications and, in particular, will further spur the interest in exploring photocatalysis with MOFs. Most MOFs also do not possess strong mechanical properties, good processability, and high electric conductivity, all of which will hinder the integration of MOFs into functional solar devices.

As a complementary alternative, more-robust molecular materials, such as cross-linked polymers that are linked through covalent C−C bonds, have recently shown potentials in solar energy utilization.[85−87] Cross-linked polymers share many of the characteristic of MOFs, such as high porosity, high chromophore/catalyst loading, structural controllability, and molecular tunability; however, they are typically amorphous materials that lack long-range orders, making the elucidation of their structure/property relationships much more difficult. On the other hand, cross-linked polymers exhibit superior stability, thus providing an alternative robust platform for designing light-harvesting and photocatalytic systems. Lin and co-workers have recently demonstrated the construction of photoactive porous or nonporous cross-linked polymers for highly efficient light-harvesting and photocatalysis.[85−87]

Although still in their infancy, photoactive MOFs have shown interesting potential in solar energy utilization. They provide a promising platform to integrate different functional molecular components to achieve light-harvesting and photocatalysis and are expected to receive increasing attention from both synthetic chemists and material scientists. Further development of MOFs and related cross-linked polymers should lead to novel molecular materials with hierarchical organizations for artificial photosynthesis.

## AUTHOR INFORMATION


### Corresponding Author

*E-mail: wlin@unc.edu.

### Author Contributions

†These authors contributed equally.


### Notes

The authors declare no competing financial interest.

## ACKNOWLEDGMENTS

This work is supported as part of the UNC EFRC: Solar Fuels, an Energy Frontier Research Center funded by the U.S. Department of Energy, Office of Science, Office of Basic Energy Sciences under Award No. DE-SC0001011 (for supporting J.W. and W.L.). C.W. acknowledges support from the NSF (DMR-0906662) and from the UNC Department of Chemistry for an Ernest L. Eliel fellowship and a Venable award.

## REFERENCES


(1) Gust, D.; Moore, T. A.; Moore, A. L. *Acc. Chem. Res.* **2009**, *42*, 1890.
(2) Barber, J. *Chem. Soc. Rev.* **2009**, *38*, 185.
(3) Dau, H.; Zaharieva, I. *Acc. Chem. Res.* **2009**, *42*, 1861.
(4) Fujishima, A.; Honda, K. *Nature* **1972**, *238*, 37.
(5) Nozik, A. J.; Beard, M. C.; Luther, J. M.; Law, M.; Ellingson, R. J.; Johnson, J. C. *Chem. Rev.* **2010**, *110*, 6873.
(6) Ohno, T.; Bai, L.; Hisatomi, T.; Maeda, K.; Domen, K. *J. Am. Chem. Soc.* **2012**, *134*, 8254.
(7) Zhang, F.; Yamakata, A.; Maeda, K.; Moriya, Y.; Takata, T.; Kubota, J.; Teshima, K.; Oishi, S.; Domen, K. *J. Am. Chem. Soc.* **2012**, *134*, 8348.
(8) Reece, S. Y.; Hamel, J. A.; Sung, K.; Jarvi, T. D.; Esswein, A. J.; Pijpers, J. J. H.; Nocera, D. G. *Science* **2011**, *334*, 645.
(9) Youngblood, W. J.; Lee, S.-H. A.; Kobayashi, Y.; Hernandez-Pagan, E. A.; Hoertz, P. G.; Moore, T. A.; Moore, A. L.; Mallouk, T. E. *J. Am. Chem. Soc.* **2009**, *131*, 926.
(10) Ledney, M.; Dutta, P. K. *J. Am. Chem. Soc.* **1995**, *117*, 7687.
(11) Wei, X.; Wang, K.-X.; Guo, X.-X.; Chen, J.-S. *Proc. R. Soc. A* **2012**, *468*, 2099.
(12) Wasielewski, M. R. *Acc. Chem. Res.* **2009**, *42*, 1910.
(13) Guldi, D. M. *Chem. Soc. Rev.* **2002**, *31*, 22.
(14) Maeda, K.; Teramura, K.; Lu, D.; Takata, T.; Saito, N.; Inoue, Y.; Domen, K. *Nature* **2006**, *440*, 295.
(15) Utschig, L. M.; Silver, S. C.; Mulfort, K. L.; Tiede, D. M. *J. Am. Chem. Soc.* **2011**, *133*, 16334.
(16) Xuan, J.; Xiao, W.-J. *Angew. Chem., Int. Ed.* **2012**, *51*, 6828.
(17) O'Keeffe, M.; Yaghi, O. M. *Chem. Rev.* **2011**, *112*, 675.
(18) Evans, O. R.; Lin, W. *Acc. Chem. Res.* **2002**, *35*, 511.
(19) Wang, C.; Zhang, T.; Lin, W. *Chem. Rev.* **2011**, *112*, 1084.
(20) Sumida, K.; Rogow, D. L.; Mason, J. A.; McDonald, T. M.; Bloch, E. D.; Herm, Z. R.; Bae, T.-H.; Long, J. R. *Chem. Rev.* **2011**, *112*, 724.
(21) Wu, H.; Gong, Q.; Olson, D. H.; Li, J. *Chem. Rev.* **2012**, *112*, 836.
(22) Cui, Y.; Yue, Y.; Qian, G.; Chen, B. *Chem. Rev.* **2011**, *112*, 1126.
(23) Kreno, L. E.; Leong, K.; Farha, O. K.; Allendorf, M.; Van Duyne, R. P.; Hupp, J. T. *Chem. Rev.* **2011**, *112*, 1105.
(24) Yoon, M.; Srirambalaji, R.; Kim, K. *Chem. Rev.* **2011**, *112*, 1196.
(25) Ma, L.; Abney, C.; Lin, W. *Chem. Soc. Rev.* **2009**, *38*, 1248.
(26) Della Rocca, J.; Liu, D.; Lin, W. *Acc. Chem. Res.* **2011**, *44*, 957.
(27) Huxford, R. C.; Della Rocca, J.; Lin, W. *Curr. Opin. Chem. Biol.* **2010**, *14*, 262.
(28) Farrusseng, D.; Aguado, S.; Pinel, C. *Angew. Chem., Int. Ed.* **2009**, *48*, 7502−7513.
(29) Van Bergen, T. J.; Hedstrand, D. M.; Kruizinga, W. H.; Kellogg, R. M. *J. Org. Chem.* **1979**, *44*, 4953.
(30) Cermenati, L.; Richter, C.; Albini, A. *Chem. Commun.* **1998**, 805.
(31) Fagnoni, M.; Dondi, D.; Ravelli, D.; Albini, A. *Chem. Rev.* **2007**, *107*, 2725.
(32) Ravelli, D.; Dondi, D.; Fagnoni, M.; Albini, A. *Chem. Soc. Rev.* **2009**, *38*, 1999.
(33) Nicewicz, D. A.; MacMillan, D. W. C. *Science* **2008**, *322*, 77.
(34) Narayanam, J. M. R.; Stephenson, C. R. J. *Chem. Soc. Rev.* **2011**, *40*, 102.
(35) Yoon, T. P.; Ischay, M. A.; Du, J. *Nat. Chem.* **2010**, *2*, 527.
(36) Cole-Hamilton, D. J. *Science* **2003**, *299*, 1702.
(37) Benaglia, M.; Puglisi, A.; Cozzi, F. *Chem. Rev.* **2003**, *103*, 3401.

(38) Song, C. E.; Lee, S.-g. *Chem. Rev.* **2002**, *102*, 3495.
(39) Silva, C. G.; Corma, A.; García, H. *J. Mater. Chem.* **2010**, *20*, 3141.
(40) Gascon, J.; Hernández-Alonso, M. D.; Almeida, A. R.; van Klink, G. P. M.; Kapteijn, F.; Mul, G. *ChemSusChem* **2008**, *1*, 981.
(41) Dan-Hardi, M.; Serre, C.; Frot, T.; Rozes, L.; Maurin, G.; Sanchez, C.; Férey, G. *J. Am. Chem. Soc.* **2009**, *131*, 10857.
(42) Collini, E.; Wong, C. Y.; Wilk, K. E.; Curmi, P. M. G.; Brumer, P.; Scholes, G. D. *Nature* **2010**, *463*, 644.
(43) Wang, J.-L.; Yan, J.; Tang, Z.-M.; Xiao, Q.; Ma, Y.; Pei, J. *J. Am. Chem. Soc.* **2008**, *130*, 9952.
(44) Zhang, X.; Ballem, M. A.; Ahrén, M.; Suska, A.; Bergman, P.; Uvdal, K. *J. Am. Chem. Soc.* **2010**, *132*, 10391.
(45) Zhang, X.; Ballem, M. A.; Hu, Z.-J.; Bergman, P.; Uvdal, K. *Angew. Chem., Int. Ed.* **2011**, *50*, 5729.
(46) Kent, C. A.; Liu, D.; Ma, L.; Papanikolas, J. M.; Meyer, T. J.; Lin, W. *J. Am. Chem. Soc.* **2011**, *133*, 12940.
(47) Kent, C. A.; Mehl, B. P.; Ma, L.; Papanikolas, J. M.; Meyer, T. J.; Lin, W. *J. Am. Chem. Soc.* **2010**, *132*, 12767.
(48) Kent, C. A.; Liu, D.; Meyer, T. J.; Lin, W. *J. Am. Chem. Soc.* **2012**, *134*, 3991.
(49) Youngblood, W. J.; Lee, S.-H. A.; Maeda, K.; Mallouk, T. E. *Acc. Chem. Res.* **2009**, *42*, 1966.
(50) deKrafft, K. E.; Wang, C.; Lin, W. *Adv. Mater.* **2012**, *24*, 2014.
(51) Hetterscheid, D. G. H.; van der Vlugt, J. I.; de Bruin, B.; Reek, J. N. H. *Angew. Chem., Int. Ed.* **2009**, *48*, 8178.
(52) Kudo, A.; Miseki, Y. *Chem. Soc. Rev.* **2009**, *38*, 253.
(53) Kataoka, Y.; Sato, K.; Miyazaki, Y.; Masuda, K.; Tanaka, H.; Naito, S.; Mori, W. *Energy Environ. Sci.* **2009**, *2*, 397.
(54) Cavka, J. H.; Jakobsen, S.; Olsbye, U.; Guillou, N.; Lamberti, C.; Bordiga, S.; Lillerud, K. P. *J. Am. Chem. Soc.* **2008**, *130*, 13850.
(55) Gomes Silva, C.; Luz, I.; Llabrés i Xamena, F. X.; Corma, A.; García, H. *Chem.—Eur. J.* **2010**, *16*, 11133.
(56) Wang, C.; deKrafft, K. E.; Lin, W. *J. Am. Chem. Soc.* **2012**, *134*, 7211.
(57) Motoyama, S.; Makiura, R.; Sakata, O.; Kitagawa, H. *J. Am. Chem. Soc.* **2011**, *133*, 5640.
(58) Kosal, M. E.; Chou, J.-H.; Wilson, S. R.; Suslick, K. S. *Nat. Mater.* **2002**, *1*, 118.
(59) Shultz, A. M.; Farha, O. K.; Hupp, J. T.; Nguyen, S. T. *J. Am. Chem. Soc.* **2009**, *131*, 4204.
(60) Fateeva, A.; Chater, P. A.; Ireland, C. P.; Tahir, A. A.; Khimyak, Y. Z.; Wiper, P. V.; Darwent, J. R.; Rosseinsky, M. J. *Angew. Chem., Int. Ed.* **2012**, *51*, 7440.
(61) Barthelet, K.; Riou, D.; Nogues, M.; Férey, G. *Inorg. Chem.* **2003**, *42*, 1739.
(62) Jordan, P.; Fromme, P.; Witt, H. T.; Klukas, O.; Saenger, W.; Krausz, N. *Nature* **2001**, *411*, 909.
(63) Morris, A. J.; Meyer, G. J.; Fujita, E. *Acc. Chem. Res.* **2009**, *42*, 1983.
(64) Lin, W.; Frei, H. *J. Am. Chem. Soc.* **2005**, *127*, 1610.
(65) Liu, Q.; Zhou, Y.; Kou, J.; Chen, X.; Tian, Z.; Gao, J.; Yan, S.; Zou, Z. *J. Am. Chem. Soc.* **2010**, *132*, 14385.
(66) Yan, S. C.; Ouyang, S. X.; Gao, J.; Yang, M.; Feng, J. Y.; Fan, X. X.; Wan, L. J.; Li, Z. S.; Ye, J. H.; Zhou, Y.; Zou, Z. G. *Angew. Chem., Int. Ed.* **2010**, *49*, 6400.
(67) Takeda, H.; Koike, K.; Inoue, H.; Ishitani, O. *J. Am. Chem. Soc.* **2008**, *130*, 2023.
(68) Wang, C.; Xie, Z.; deKrafft, K. E.; Lin, W. *J. Am. Chem. Soc.* **2011**, *133*, 13445.
(69) Fu, Y.; Sun, D.; Chen, Y.; Huang, R.; Ding, Z.; Fu, X.; Li, Z. *Angew. Chem., Int. Ed.* **2012**, *51*, 3364.
(70) Miguel, M. d.; Ragon, F.; Devic, T.; Serre, C.; Horcajada, P.; García, H. *ChemPhysChem* **2012**, *13*, 1.
(71) Hedstrand, D. M.; Kruizinga, W. H.; Kellogg, R. M. *Tetrahedron Lett.* **1978**, *19*, 1255.
(72) Fagnoni, M.; Dondi, D.; Ravelli, D.; Albini, A. *Chem. Rev.* **2007**, *107*, 2725.
(73) Ravelli, D.; Dondi, D.; Fagnoni, M.; Albini, A. *Chem. Soc. Rev.* **2009**, *38*, 1999.
(74) Alvaro, M.; Carbonell, E.; Ferrer, B.; Llabrés i Xamena, F. X.; Garcia, H. *Chem.—Eur. J.* **2007**, *13*, 5106.
(75) Das, M. C.; Xu, H.; Wang, Z.; Srinivas, G.; Zhou, W.; Yue, Y.-F.; Nesterov, V. N.; Qian, G.; Chen, B. *Chem. Commun.* **2011**, *47*, 11715.
(76) Wen, L.; Zhao, J.; Lv, K.; Wu, Y.; Deng, K.; Leng, X.; Li, D. *Cryst. Growth Des.* **2012**, *12*, 1603.
(77) Lin, S.; Ischay, M. A.; Fry, C. G.; Yoon, T. P. *J. Am. Chem. Soc.* **2011**, *133*, 19350.
(78) Condie, A. G.; González-Gómez, J. C.; Stephenson, C. R. J. *J. Am. Chem. Soc.* **2010**, *132*, 1464.
(79) Lee, C. Y.; Farha, O. K.; Hong, B. J.; Sarjeant, A. A.; Nguyen, S. T.; Hupp, J. T. *J. Am. Chem. Soc.* **2011**, *133*, 15858.
(80) Yang, X.-L.; Xie, M.-H.; Zou, C.; He, Y.; Chen, B.; O'Keeffe, M.; Wu, C.-D. *J. Am. Chem. Soc.* **2012**, *134*, 10638.
(81) Xie, M.-H.; Yang, X.-L.; Zou, C.; Wu, C.-D. *Inorg. Chem.* **2011**, *50*, 5318.
(82) Ma, L.; Falkowski, J. M.; Abney, C.; Lin, W. *Nat. Chem.* **2010**, *2*, 838.
(83) Shih, H.-W.; Vander Wal, M. N.; Grange, R. L.; MacMillan, D. W. C. *J. Am. Chem. Soc.* **2010**, *132*, 13600.
(84) Wu, P.; He, C.; Wang, J.; Peng, X.; Li, X.; An, Y.; Duan, C. *J. Am. Chem. Soc.* **2012**, *134*, 14991.
(85) Xie, Z.; Wang, C.; deKrafft, K. E.; Lin, W. *J. Am. Chem. Soc.* **2011**, *133*, 2056.
(86) Wang, C.; Xie, Z.; deKrafft, K. E.; Lin, W. *ACS Appl. Mater. Interfaces* **2012**, *4*, 2288.
(87) Wang, J.-L.; Wang, C.; deKrafft, K. E.; Lin, W. *ACS Catal.* **2012**, *2*, 417.